EXTENSION OF THE UNSTRUCTURED ALGORITHMS OF LIOU AND STEFFEN JR. AND OF RADESPIEL AND KROLL TO SECOND ORDER ACCURACY EMPLOYING LINEAR RECONSTRUCTION AND APPLICATION TO THE EULER EQUATIONS IN 2D - THEORY

Edisson Sávio de Góes Maciel, edissonsavio@yahoo.com.br
Mechanical Engineer / Researcher – Rua Demócrito Cavalcanti, 152 – Afogados – Recife – PE – Brazil – 50750-080

Abstract. *In the present work, the Liou and Steffen Jr. and the Radespiel and Kroll schemes are implemented, on a finite volume context and using an upwind and unstructured spatial discretization, to solve the Euler equations in the two-dimensional space. Both schemes are flux vector splitting ones. These schemes are implemented in their second order accuracy versions employing the reconstruction linear method of Barth and Jespersen and their results are compared with their first order accuracy versions and with theoretical results. Five nonlinear flux limiters are studied: Barth and Jespersen (minmod like), Van Leer, Van Albada, Superbee and β-limiter. The time integration uses a Runge-Kutta method of five stages and is second order accurate. Both algorithms are accelerated to the steady state solution using a spatially variable time step procedure. This technique has proved excellent gains in terms of convergence ratio as reported in Maciel. The algorithms are applied to the solution of the steady state physical problem of the supersonic flow along a compression corner. In this paper, the first of this series (THEORY), the theories involving the numerical implementation of the two schemes to first order accuracy and later the extension to second order accuracy are developed, whereas in the second paper of this series (RESULTS), the numerical solutions obtained with both schemes, in their first and second order accuracies, are presented and analyzed. The results have shown that the Radespiel and Kroll scheme using Barth and Jespersen, Van Leer, Van Albada and Superbee nonlinear limiters presents the most accurate values to the shock angle of the oblique shock wave generated at the compression corner.*

Keywords*: Liou and Steffen Jr. algorithm, Radespiel and Kroll algorithm, Unstructured algorithms, Linear reconstruction, Euler equations.*

1. INTRODUCTION

Conventional non-upwind algorithms have been used extensively to solve a wide variety of problems (Kutler, 1975, and Steger, 1978). Conventional algorithms are somewhat unreliable in the sense that for every different problem (and sometimes, every different case in the same class of problems) artificial dissipation terms must be specially tuned and judicially chosen for convergence. Also, complex problems with shocks and steep compression and expansion gradients may defy solution altogether.

Upwind schemes are in general more robust but are also more involved in their derivation and application. Some upwind schemes that have been applied to the Euler equations are reported below.

Liou and Steffen Jr. (1993) proposed a new flux vector splitting scheme. They declared that their scheme was simple and its accuracy was equivalent and, in some cases, better than the Roe (1981) scheme accuracy in the solutions of the Euler and the Navier-Stokes equations. The scheme was robust and converged solutions were obtained so fast as the Roe (1981) scheme. The authors proposed the approximated definition of an advection Mach number at the cell face, using its neighbor cell values via associated characteristic velocities. This interface Mach number was so used to determine the upwind extrapolation of the convective quantities.

Radespiel and Kroll (1995) emphasized that the Liou and Steffen Jr. (1993) scheme had its merits of low computational complexity and low numerical diffusion as compared to other methods. They also mentioned that the original method had several deficiencies. The method yielded local pressure oscillations in the shock wave proximities, adverse mesh and flow alignment problems. In the Radespiel and Kroll (1995) work, a hybrid flux vector splitting scheme, which alternated between the Liou and Steffen Jr. (1993) scheme and the Van Leer (1982) scheme, in the shock wave regions, is proposed, assuring that resolution of strength shocks was clear and sharply defined.

Algorithms for solving the Euler equations using a perfect gas model on structured grids in two- and three-dimensions have become widespread in recent years (Turkel and Van Leer, 1984, and Riggins, Walters and Pelletier, 1988). However, these algorithms have shown difficulties in predicting satisfactory results around complex geometries due to mesh irregularities. As a result, attention has turned to the development of solution algorithms on arbitrary unstructured grids. Impressive results have been obtained for a wide range of problems (Mavriplis and Jameson, 1987, and Barth and Jespersen, 1989).

One problem associated with unstructured meshes is the increased difficulty in obtaining smooth higher order spatial approximations to state data at cell interfaces. Two methods have been used to obtain higher order accuracy on unstructured meshes. A method used by several researchers for cell vertex schemes (Stoufflet *et al*., 1987, and Whitaker, 1988) was applied to obtain higher order accuracy in a procedure analogous to MUSCL differencing on a

structured mesh. A conventional structured mesh limiter can be employed in this scheme to obtain approximately monotone results near flow discontinuities. The second method, which was proposed by Barth and Jespersen (1989), linearly reconstructs the cell averaged data and imposes a monotone preserving limiter to achieve smooth results near flow discontinuities.

On an unstructured algorithm context, Maciel (2007a,b) have presented a work involving the numerical implementation of four typical algorithms of the Computational Fluid Dynamics community. The Roe (1981), the Steger and Warming (1981), the Van Leer (1982) and the Harten (1983) algorithms were implemented and applied to the solution of aeronautical and of aerospace problems, in two-dimensions. The Euler equations in conservative form, employing a finite volume formulation and an unstructured spatial discretization, were solved. The Roe (1981) and the Harten (1983) schemes were flux difference splitting ones and more accurate solutions were expected. On the other hand, the Steger and Warming (1981) and the Van Leer (1982) schemes were flux vector splitting ones and more robustness properties were expected. The time integration was performed by a Runge-Kutta method of five stages. All four schemes were first order accurate in space and second order accurate in time. The steady state physical problems of the transonic flow along a convergent-divergent nozzle and of the supersonic flows along a ramp and around a blunt body were studied. The results have shown that the Roe (1981) scheme has presented the most severe pressure fields in the ramp and blunt body problems and the most accurate value of the stagnation pressure in the blunt body case. On the other hand, the Van Leer (1982) scheme has yielded the most accurate value of the shock angle in the ramp problem, while the Harten (1983) scheme has yielded the best value of the lift coefficient in the blunt body problem.

Following the studies of 2007, Maciel (2008a,b) have presented a work involving the numerical implementation of more three typical algorithms of the Computational Fluid Dynamics community. The Frink, Parikh and Pirzadeh (1991), the Liou and Steffen Jr. (1993), and the Radespiel and Kroll (1995) algorithms were implemented and applied to the solution of aeronautical and aerospace problems, in two-dimensions. The Euler equations in conservative form, employing a finite volume formulation and an unstructured spatial discretization, were solved. The Frink, Parikh and Pirzadeh (1991) scheme was a flux difference splitting one and more accurate solutions were expected. On the other hand, the Liou and Steffen Jr. (1993) and the Radespiel and Kroll (1995) schemes were flux vector splitting ones and more robustness properties were expected. The time integration was performed by a Runge-Kutta method of five stages. All three schemes were first order accurate in space and second order accurate in time. The steady state physical problems of the transonic flow along a convergent-divergent nozzle, of the supersonic flows along a ramp and around a blunt body, and of the "cold gas" hypersonic flow around a double ellipse were studied. The results have shown that the Frink, Parikh and Pirzadeh (1991) scheme presents the most severe pressure fields and the most accurate values of the stagnation pressure in the blunt body and in the double ellipse problems. On the other hand, the Liou and Steffen Jr. (1993) scheme yields the best wall pressure distribution, in comparison with the experimental results, in the nozzle problem, while the Radespiel and Kroll (1995) scheme yields the most accurate value of the shock angle in the ramp problem.

In the present work, the Liou and Steffen Jr. (1993) and the Radespiel and Kroll (1995) schemes are implemented, on a finite volume context and using an upwind and unstructured spatial discretization, to solve the Euler equations in the two-dimensional space. Both schemes are flux vector splitting ones. These schemes are implemented in their second order accuracy versions employing the reconstruction linear method of Barth and Jespersen (1989) and their results are compared with their first order accuracy versions and with theoretical results. Five nonlinear flux limiters are studied: Barth and Jespersen (minmod like), Van Leer, Van Albada, Superbee and β-limiter. The time integration uses a Runge-Kutta method of five stages and is second order accurate. Both algorithms are accelerated to the steady state solution using a spatially variable time step. This technique has proved excellent gains in terms of convergence ratio as reported in Maciel (2005 and 2008c). The algorithms are applied to the solution of the steady state physical problem of the supersonic flow along a compression corner.

In this paper, the first of this series (THEORY), the theories involving the numerical implementation of the two schemes to first order accuracy and later the extension to second order accuracy are developed, whereas in the second paper of this series (RESULTS), the numerical solutions obtained with both schemes, in their first and second order accuracies, are presented and analyzed. The results have shown that the Radespiel and Kroll (1995) scheme using Barth and Jespersen, Van Leer, Van Albada and Superbee nonlinear limiters presents the most accurate values to the shock angle of the oblique shock wave generated at the compression corner.

An unstructured discretization of the calculation domain is usually recommended to complex configurations, due to the easily and efficiency that such domains can be discretized (Mavriplis, 1990, and Pirzadeh, 1991). However, the unstructured mesh generation question will not be studied in this work.

2. EULER EQUATIONS

The fluid movement is described by the Euler equations, which express the conservation of mass, of linear momentum and of energy to an inviscid mean, heat non-conductor and compressible, in the absence of external forces. In integral and conservative forms, these equations can be represented by:

$$\partial/\partial t \int_V Q \, dV + \int_S \left[(E_e) n_x + (F_e) n_y \right] dS = 0, \tag{1}$$

with Q written to a Cartesian system, V is the cell volume, n_x and n_y are the components of the normal unity vector to the flux face, S is the flux area, and E_e and F_e are the convective flux vector components. The Q, E_e and F_e vectors are represented by:

$$Q = \begin{Bmatrix} \rho \\ \rho u \\ \rho v \\ e \end{Bmatrix}, \quad E_e = \begin{Bmatrix} \rho u \\ \rho u^2 + p \\ \rho uv \\ (e+p)u \end{Bmatrix} \quad \text{and} \quad F_e = \begin{Bmatrix} \rho v \\ \rho uv \\ \rho v^2 + p \\ (e+p)v \end{Bmatrix}, \tag{2}$$

being ρ the fluid density; u and v the Cartesian components of the velocity vector in the x and y directions, respectively; e the fluid total energy; and p the fluid static pressure.

In the studied problem, the Euler equations were nondimensionalized in relation to the freestream density, ρ_∞, and in relation to the freestream speed of sound, a_∞. Hence, the density is nondimensionalized in relation to ρ_∞; the u and v velocity components are nondimensionalized in relation to a_∞; and the pressure and the total energy are nondimensionalized in relation to the product $\rho_\infty (a_\infty)^2$. The matrix system of the Euler equations is closed with the state equation

$$p = (\gamma - 1) \left[e - 0.5 \rho (u^2 + v^2) \right], \tag{3}$$

assuming the ideal gas hypothesis. γ is the ratio of specific heats, equal to 1.4 to air. The total enthalpy is determined by

$$H = (e + p)/\rho. \tag{4}$$

3. LIOU AND STEFFEN JR. (1993) ALGORITHM

The approximation of the integral equation (1) to a triangular finite volume yields a system of ordinary differential equations with respect to time:

$$V_i \, dQ_i / dt = -C_i, \tag{5}$$

with C_i representing the net flux (residual) of conservation of mass, of linear momentum and of energy in the V_i volume. The residual is calculated according to:

$$C_i = F_1 + F_2 + F_3, \tag{6}$$

where F_l is the discrete convective flux at the interface "l".

As shown in Liou and Steffen Jr. (1993), the discrete convective flux calculated by the AUSM scheme ("Advection Upstream Splitting Method") can be interpreted as a sum involving the arithmetical average between the right (R) and the left (L) states of the "l" cell face, multiplied by the interface Mach number, and a scalar dissipative term. The subscript "L" is associated to properties of a given "i" cell and the subscript "R" is associated to properties of the "ne" neighbor cell of "i". Hence, to the "l" interface:

$$F_l = |S|_l \left(\frac{1}{2} M_l \left(\begin{bmatrix} \rho a \\ \rho au \\ \rho av \\ \rho aH \end{bmatrix}_L + \begin{bmatrix} \rho a \\ \rho au \\ \rho av \\ \rho aH \end{bmatrix}_R \right) - \frac{1}{2} \phi_l \left(\begin{bmatrix} \rho a \\ \rho au \\ \rho av \\ \rho aH \end{bmatrix}_R - \begin{bmatrix} \rho a \\ \rho au \\ \rho av \\ \rho aH \end{bmatrix}_L \right) \right) + \begin{bmatrix} 0 \\ S_x p \\ S_y p \\ 0 \end{bmatrix}_l, \tag{7}$$

where $S_l = \begin{bmatrix} S_x & S_y \end{bmatrix}_l^T$ defines the normal area vector to the "l" surface. The area components at this interface are defined by:

$$S_x^l = n_x^l S^l \quad \text{and} \quad S_y^l = n_y^l S^l. \tag{8}$$

The normal unity vector components, n_x^l and n_y^l, and the flux area of the "l" interface, S^l, are defined as:

$$n_x^l = \Delta y_l \Big/ \left(\Delta x_l^2 + \Delta y_l^2 \right)^{0.5}, \quad n_y^l = -\Delta x_l \Big/ \left(\Delta x_l^2 + \Delta y_l^2 \right)^{0.5} \quad \text{and} \quad S^l = \left(\Delta x_l^2 + \Delta y_l^2 \right)^{0.5}. \tag{9}$$

Expressions to Δx_l and Δy_l are given in Tab. 1. Figure 1 illustrates the "i" volume and its respective neighbors, its nodes and its flux interfaces.

Table 1. Values of Δx_l and Δy_l.

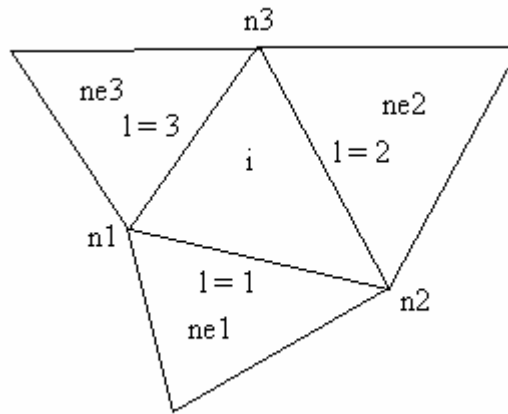| Interface	Δx_l	Δy_l
$l = 1$	$x_{n2} - x_{n1}$	$y_{n2} - y_{n1}$
$l = 2$	$x_{n3} - x_{n2}$	$y_{n3} - y_{n2}$
$l = 3$	$x_{n1} - x_{n3}$	$y_{n1} - y_{n3}$

Figure 1. Schematic of a cell and its neighbors, nodes and flux interfaces.

The "a" quantity represents the speed of sound, defined as $a = \sqrt{\gamma p / \rho}$. M_l defines the advection Mach number at the "l" face of the "i" cell, which is calculated according to Liou and Steffen Jr. (1993) as:

$$M_l = M_L^+ + M_R^-, \tag{10}$$

where the separated Mach numbers $M^{+/-}$ are defined by the Van Leer (1982) formulas:

$$M^+ = \begin{bmatrix} M, & \text{if } M \geq 1; \\ 0.25(M+1)^2, & \text{if } |M| < 1; \quad \text{and} \\ 0, & \text{if } M \leq -1; \end{bmatrix} \quad M^- = \begin{bmatrix} 0, & \text{if } M \geq 1; \\ -0.25(M-1)^2, & \text{if } |M| < 1; \\ M, & \text{if } M \leq -1. \end{bmatrix} \tag{11}$$

M_L and M_R represent the Mach number associated with the left and right states, respectively. The advection Mach number is defined by:

$$M = \left(S_x u + S_y v \right) \Big/ \left(|S| a \right). \tag{12}$$

The pressure at the "l" face of the "i" cell is calculated by a similar way:

$$p_l = p_L^+ + p_R^-, \tag{13}$$

with $p^{+/-}$ denoting the pressure separation defined according to the Van Leer (1982) formulas:

$$p^+ = \begin{bmatrix} p, & if\ M \geq 1; \\ 0.25p(M+1)^2(2-M), & if\ |M| < 1 \\ 0, & if\ M \leq -1; \end{bmatrix} \quad and \quad p^- = \begin{bmatrix} 0, & if\ M \geq 1; \\ 0.25p(M-1)^2(2+M), & if\ |M| < 1; \\ p, & if\ M \leq -1. \end{bmatrix} \quad (14)$$

The definition of the dissipative term ϕ determines the particular formulation of the convective fluxes. According to Radespiel and Kroll (1995), the choice below corresponds to the Liou and Steffen Jr. (1993) scheme:

$$\phi_l = \phi_l^{LS} = |M_l|. \quad (15)$$

The equations above clearly show that to a supersonic Mach number at the cell face, the Liou and Steffen Jr. (1993) scheme represents a purely upwind discretization, using either the left state or the right state to the convective and pressure terms, depending of the Mach number signal.

The time integration is performed by a Runge-Kutta explicit method of five stages, second order accurate, and can be represented in general form by:

$$Q_i^{(0)} = Q_i^{(n)}$$
$$Q_i^{(k)} = Q_i^{(0)} - \alpha_k\ \Delta t_i / V_i \times C\left(Q_i^{(k-1)}\right), \quad (16)$$
$$Q_i^{(n+1)} = Q_i^{(k)}$$

with $k = 1,...,5$; $\alpha_1 = 1/4$, $\alpha_2 = 1/6$, $\alpha_3 = 3/8$, $\alpha_4 = 1/2$ and $\alpha_5 = 1$; and $C = F_1+F_2+F_3$. The cell volume on an unstructured context is defined by:

$$V_i = 0.5|(x_{n1}y_{n2} + y_{n1}x_{n3} + x_{n2}y_{n3}) - (x_{n3}y_{n2} + y_{n3}x_{n1} + x_{n2}y_{n1})|, \quad (17)$$

with n_1, n_2 and n_3 being the nodes of a given triangular cell, defined in Fig. 1. This version of the Liou and Steffen Jr. (1993) scheme is first order accurate in space.

4. RADESPIEL AND KROLL (1995) ALGORITHM

The Radespiel and Kroll (1995) scheme is described by Eqs. (5) to (14). The next step is the determination of the ϕ dissipative term. A hybrid scheme is proposed by Radespiel and Kroll (1995), which combines the Van Leer (1982) scheme and the Liou and Steffen Jr. (1993) (AUSM) scheme. Hence,

$$\phi_l = (1-\omega)\phi_l^{VL} + \omega\phi_l^{LS}, \quad (18)$$

with:

$$\phi_l^{VL} = \begin{cases} |M_l|, & if\ |M_l| \geq 1; \\ |M_l| + \frac{1}{2}(M_R - 1)^2, & if\ 0 \leq M_l < 1; \\ |M_l| + \frac{1}{2}(M_L + 1)^2, & if\ -1 < M_l \leq 0; \end{cases} \quad and \quad \phi_l^{LS} = \begin{cases} |M_l|, & if\ |M_l| \geq \tilde{\delta} \\ \frac{(M_l)^2 + \tilde{\delta}^2}{2\tilde{\delta}}, & if\ |M_l| < \tilde{\delta} \end{cases}, \quad (19)$$

where $\tilde{\delta}$ is a small parameter, $0 < \tilde{\delta} \leq 0.5$, and ω is a constant, $0 \leq \omega \leq 1$. In this work, the values used to $\tilde{\delta}$ and ω were: 0.2 and 0.5, respectively. It is important to note that $\omega = 1$ and $\tilde{\delta} = 0$ recover the Liou and Steffen Jr. (1993) scheme. The time integration follows the method described by Eq. (16). This scheme is first order accurate in space.

5. CELL CENTERED HIGHER ORDER CORRECTION

A piecewise linear redistribution of the cell averaged flow variables to obtain higher order accuracy while insuring that new extrema are not created in the reconstruction process is given by Barth and Jespersen (1989) as

$$Q(x, y) = Q(x_0, y_0) + \nabla Q \bullet r = Q(x_0, y_0) + Q_x[x - x_0] + Q_y[y - y_0], \tag{20}$$

where r is the vector from the cell center (x_0, y_0) to any point (x,y) in the cell, and ∇Q represents the solution gradient in the cell. Note that this equation is simply the first order accurate Taylor approximation plus a higher order correction. With this approximation, the solution gradient ∇Q is constant in each cell and can be computed from

$$\nabla Q_i = \frac{1}{V_\Omega} \oint_\Omega (Q.n) d\Omega, \tag{21}$$

where V_Ω is the volume contained in the path of integration. For the cell centered case, the path chosen passes through the centroids "a", "b" and "c" of the three surrounding cells "$ne1$", "$ne2$" and "$ne3$" of the given cell "i", respectively, as shown in Fig. 2. The vector ∇Q represents the best estimate of the solution gradient in the cell computed from surrounding centroid data.
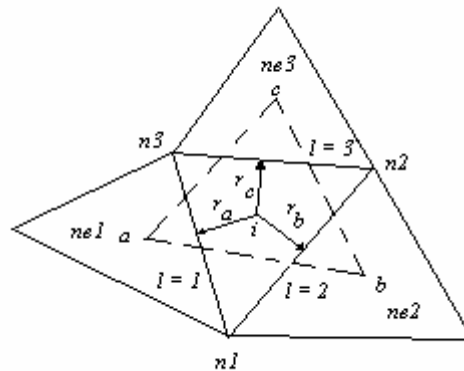

Figure 2. Integration path for the gradient calculation of cell centered case.

Consider a limited version of the linear function about the centroid of cell i

$$Q(x, y)_i = Q(x_0, y_0) + \Phi_i \nabla Q_i \bullet r_i, \qquad \Phi_i \ \varepsilon \ [0,1]. \tag{22}$$

To find the value of Φ_i, a monotonicity principle is enforced on the unlimited quantities $Q_{i_n} = Q(x_n, y_n)_i$ calculated in Eq. (20) at the faces of cell "i". It requires that the values computed at the faces must not exceed the maximum and minimum of neighboring centroid values, including the centroid value in cell "i", i.e., that

$$Q_i^{min} \le Q_{i_n} \le Q_i^{max}, \tag{23}$$

where $Q_i^{min} = \min(Q_i, Q_{neighbors})$ and $Q_i^{max} = \max(Q_i, Q_{neighbors})$. Note that this definition differs from that of Harten, Hyman and Lax (1976), but coincides with the monotonicity definition used recently by Spekreijse (1987) for structured meshes in multi-dimensions. For linear reconstructions, extrema in $Q(x,y)_i$ occur at the vertices of the face and sufficient conditions for Eq. (22) can be easily obtained. The value Φ_i can now be calculated for each vertex j of cell i as

$$s = \begin{cases} \dfrac{Q_i^{max} - Q_i}{Q_j - Q_i}, & if \quad Q_j - Q_i > 0; \\ \dfrac{Q_i^{min} - Q_i}{Q_j - Q_i}, & if \quad Q_j - Q_i < 0; \qquad \overline{\Phi}_{i_j} = \min(1, s), \\ 1, & if \quad Q_j - Q_i = 0; \end{cases} \tag{24}$$

with $\Phi_i = \min\left(\overline{\Phi}_{i_1}, \overline{\Phi}_{i_2}, \overline{\Phi}_{i_3}\right)$, where "$j$" is the index of each vertex defining cell "i". New limited values for Q_i at each of the faces of cell "i" are then calculated from Eq. (22) using the value of Φ_i calculated for the cell. Following this procedure guarantees that the linearly reconstructed state variables satisfy the monotonicity principle when evaluated

anywhere within a face. The nonlinear limiter described by Eq. (24) is of a minmod type. Other limiters are presented below and were studied in this work. The definitions of these limiters are presented in Hirsch (1990).

- Van Leer nonlinear limiter:

$$\overline{\Phi}_{i_j} = \frac{s + |s|}{1 + s} ; \tag{25}$$

- Van Albada nonlinear limiter:

$$\overline{\Phi}_{i_j} = \frac{s + s^2}{1 + s^2} ; \tag{26}$$

- Superbee nonlinear limiter:

$$\overline{\Phi}_{i_j} = \max\left[0, \min(2s, 1), \min(s, 2)\right] ; \tag{27}$$

- β-limiter:

$$\overline{\Phi}_{i_j} = \max\left[0, \min(\beta s, 1), \min(s, \beta)\right] , \tag{28}$$

where "s" is the ratio of differences of the components of the vector of conserved variables, defined according to Eq. (24), and β assumes values from 1.0 to 2.0, being 1.5 the value adopted in this work.

6. SPATIALLY VARIABLE TIME STEP

The basic idea of this procedure consists in keeping constant the CFL number in all calculation domain, allowing, hence, the use of appropriated time steps to each specific mesh region during the convergence process. Hence, according to the definition of the CFL number, it is possible to write:

$$\Delta t_i = CFL(\Delta s)_i / c_i , \tag{29}$$

where: CFL is the "Courant-Friedrichs-Lewy" number to provide numerical stability to the scheme; $c_i = \left[\left(u^2 + v^2\right)^{0.5} + a\right]_i$ is the maximum characteristic velocity of information propagation in the calculation domain; and $(\Delta s)_i$ is a characteristic length of information transport. On a finite volume context, $(\Delta s)_i$ is chosen as the minor value found between the minor centroid distance, involving the "i" cell and a neighbor, and the minor cell side length.

7. INITIAL AND BOUNDARY CONDITIONS

7.1. Initial condition

To the compression corner problem, values of freestream flow are adopted for all properties as initial condition, in the whole calculation domain (Jameson and Mavriplis, 1986, Maciel, 2002, and Maciel, 2008a). Therefore, the vector of conserved variables is defined as:

$$Q_i = \left\{ 1 \quad M_\infty \cos\alpha \quad M_\infty \sin\alpha \quad \frac{1}{\gamma(\gamma - 1)} + 0.5 M_\infty^2 \right\}^T , \tag{30}$$

being M_∞ the freestream flow Mach number and α the flow attack angle.

7.2. Boundary conditions

The boundary conditions are basically of three types: solid wall, entrance and exit. These conditions are implemented in special cells named ghost cells.

(a) Wall condition: This condition imposes the flow tangency at the solid wall. This condition is satisfied considering the wall tangent velocity component of the ghost volume as equals to the respective velocity component of its real neighbor cell. At the same way, the wall normal velocity component of the ghost cell is equaled in value, but with opposite signal, to the respective velocity component of the real neighbor cell.

The pressure gradient normal to the wall is assumed to be equal to zero, following an inviscid formulation. The same hypothesis is applied to the temperature gradient normal to the wall, which corresponds to an adiabatic condition. The ghost volume density and pressure are extrapolated from the respective values of the real neighbor volume (zero order extrapolation), with these two conditions. The total energy is obtained by the state equation of a perfect gas.

(b) Entrance condition:

(b.1) Subsonic flow: Three properties are specified and one is extrapolated, based on analysis of information propagation along characteristic directions in the calculation domain (Maciel, 2002). In other words, three characteristic directions of information propagation point inward the computational domain and should be specified, to the subsonic flow. Only the characteristic direction associated to the "(q_n-a)" velocity cannot be specified and should be determined by interior information of the calculation domain. The pressure was the extrapolated variable from the real neighbor volume, to the studied problem. Density and velocity components had their values determined by the freestream flow properties. The total energy per unity fluid volume is determined by the state equation of a perfect gas.

(b.2) Supersonic flow: All variables are fixed with freestream flow values, at the boundary entrance.

(c) Exit condition:

(c.1) Subsonic flow: Three characteristic directions of information propagation point outward the computational domain and should be extrapolated from interior information. The characteristic direction associated to the "(q_n-a)" velocity should be specified because it penetrates the calculation domain (Maciel, 2002). In this case, the ghost volume's pressure is specified by its initial value. Density and velocity components are extrapolated and the total energy is obtained by the state equation of a perfect gas.

(c.2) Supersonic flow: All variables are extrapolated from the interior domain due to the fact that all four characteristic directions of information propagation of the Euler equations point outward the calculation domain and, with it, nothing can be fixed.

8. CONCLUSIONS

In the present work, the Liou and Steffen Jr. (1993) and the Radespiel and Kroll (1995) schemes are implemented, on a finite volume context and using an upwind and unstructured spatial discretization, to solve the Euler equations in the two-dimensional space. Both schemes are flux vector splitting ones. These schemes are implemented in their second order accuracy versions employing the reconstruction linear method of Barth and Jespersen (1989) and their results are compared with their first order accuracy versions and with theoretical results. Five nonlinear flux limiters are studied: Barth and Jespersen (minmod like), Van Leer, Van Albada, Superbee and β-limiter. The time integration uses a Runge-Kutta method of five stages and is second order accurate. Both algorithms are accelerated to the steady state solution using a spatially variable time step. This technique has proved excellent gains in terms of convergence ratio as reported in Maciel (2005 and 2008c). The algorithms are applied to the solution of the steady state physical problem of the supersonic flow along a compression corner.

In this paper, the first of this series (THEORY), the theories involving the numerical implementation of the two schemes to first order accuracy and later the extension to second order accuracy are developed, whereas in the second paper of this series (RESULTS), the numerical solutions obtained with both schemes, in their first and second order accuracies, are presented and analyzed. The results have shown that the Radespiel and Kroll (1995) scheme using Barth and Jespersen, Van Leer, Van Albada and Superbee nonlinear limiters presents the most accurate values to the shock angle of the oblique shock wave generated at the compression corner.

9. ACKNOWLEDGEMENTS

10. REFERENCES

Barth, T. J., and Jespersen, D. C., 1989, "The Design and Application of Upwind Schemes on Unstructured Meshes", AIAA Paper 89-0336.

Frink, N. T., Parikh, P., and Pirzadeh, S., 1991, "Aerodynamic Analysis of Complex Configurations Using Unstructured Grids", AIAA 91-3292-CP.

Harten, A., 1983, "High Resolution Schemes for Hyperbolic Conservation Laws", Journal of Computational Physics, Vol. 49, pp. 357-393.

Harten, A., Hyman, J., and Lax, P., 1976, "On Finite-Difference Approximations and Entropy Conditions for Shocks", Comm. Pure Appl. Math., Vol. 29.

Hirsch, C., 1990, "Numerical Computation of Internal and External Flows – Computational Methods for Inviscid and Viscous Flows", John Wiley & Sons Ltd, 691p.

Jameson, A., and Mavriplis, D., 1986, "Finite Volume Solution of the Two-Dimensional Euler Equations on a Regular Triangular Mesh, AIAA Journal, Vol. 24, No. 4, pp. 611-618.

Kutler, P., 1975, "Computation of Three-Dimensional, Inviscid Supersonic Flows", Lecture Notes in Physics, Vol. 41, pp. 287-374.

Liou, M., and Steffen Jr., C. J., 1993, "A New Flux Splitting Scheme", Journal of Computational Physics, Vol. 107, pp. 23-39.

Maciel, E. S. G., 2002, "Simulação Numérica de Escoamentos Supersônicos e Hipersônicos Utilizando Técnicas de Dinâmica dos Fluidos Computacional", Doctoral Thesis, ITA, CTA, São José dos Campos, SP, Brazil, 258 p.

Maciel, E. S. G., 2005, "Analysis of Convergence Acceleration Techniques Used in Unstructured Algorithms in the Solution of Aeronautical Problems – Part I", Proceedings of the XVIII International Congress of Mechanical Engineering (XVIII COBEM), Ouro Preto, MG, Brazil.

Maciel, E. S. G., 2007a, "Comparison Between the First Order Upwind Unstructured Algorithms of Roe and of Harten in the Solution of the Euler Equations in Two-Dimensions", Proceedings of the XIX Congress of Mechanical Engineering (XIX COBEM), Brasília, DF, Brazil.

Maciel, E. S. G., 2007b, "Comparison Between the First Order Upwind Unstructured Algorithms of Steger and Warming and of Van Leer in the Solution of the Euler Equations in Two-Dimensions", Proceedings of the XIX Congress of Mechanical Engineering (XIX COBEM), Brasília, DF, Brazil.

Maciel, E. S. G., 2008a, "Comparison Among the Unstructured Algorithms of Frink, Parikh and Pirzadeh, of Liou and Steffen, and of Radespiel and Kroll in the Solution of the Euler Equations in 2D - Theory", Proceedings of the 8th Symposium of Computational Mechanics (VIII SIMMEC), Belo Horizonte, MG, Brasil.

Maciel, E. S. G., 2008b, "Comparison Among the Unstructured Algorithms of Frink, Parikh and Pirzadeh, of Liou and Steffen, and of Radespiel and Kroll in the Solution of the Euler Equations in 2D - Results", Proceedings of the 8th Symposium of Computational Mechanics (VIII SIMMEC), Belo Horizonte, MG, Brasil.

Maciel, E. S. G., 2008c, "Analysis of Convergence Acceleration Techniques Used in Unstructured Algorithms in the Solution of Aerospace Problems – Part II", Proceedings of the XII Brazilian Congress of Thermal Engineering and Sciences (XII ENCIT), Belo Horizonte, MG, Brazil.

Mavriplis, D. J., 1990, "Accurate Multigrid Solution of the Euler Equations on Unstructured and Adaptive Meshes", AIAA Journal, Vol. 28, No. 2, pp. 213-221.

Mavriplis, D., and Jameson, A., 1987, "Multigrid Solution of the Euler Equations on Unstructured and Adaptive Meshes", ICASE Report. 87-53; also NASA CR 178346.

Pirzadeh, S., 1991, "Structured Background Grids for Generation of Unstructured Grids by Advancing Front Method", AIAA Paper 91-3233-CP.

Radespiel, R., and Kroll, N., 1995, "Accurate Flux Vector Splitting for Shocks and Shear Layers", Journal of Computational Physics, Vol. 121, pp. 66-78.

Riggins, D. W., Walters, R. W., and Pelletier, D., 1988, "The use of Direct Solvers for Compressible Flow Computations", AIAA Paper 88-0229.

Roe, P. L., 1981, "Approximate Riemann Solvers, Parameter Vectors, and Difference Schemes", Journal of Computational Physics, Vol. 43, pp. 357-372.

Spekreijse, S. P., 1987, "Multigrid Solution of the Steady Euler Equations", Doctoral Thesis, Deft University of Technology.

Steger, J. L., 1978, "Implicit Finite-Difference Simulation of Flow About Arbitrary Two-Dimensional Geometries", AIAA Journal, Vol. 16, No. 7, pp. 679-686.

Steger, J. L. and Warming, R. F., 1981, "Flux Vector Splitting of the Inviscid Gasdynamic Equations with Application to Finite-Difference Methods", Journal of Computational Physics, Vol. 40, pp. 263-293.

Stoufflet, B., Périaux, J., Fezoui, F., and Dervieux, A., 1987, "Numerical Simulation of 3-D Hypersonic Euler Flows Around Space Vehicles Using Adapted Finite-Elements", AIAA Paper 87-0560.

Turkel, E., and Van Leer, B., 1984, "Flux-Vector Splitting and Runge-Kutta Methods for the Euler Equations", ICASE Report 84-27; also NASA CR 172415.

Van Leer, B., 1982, "Flux-Vector Splitting for the Euler Equations", Proceedings of the 8th International Conference on Numerical Methods in Fluid Dynamics, E. Krause, Editor, Lecture Notes in Physics, Vol. 70, pp. 507-512, Springer-Verlag, Berlin.

Whitaker, D. L., 1988, "Two-Dimensional Euler Computations on a Triangular Mesh Using an Upwind, Finite-Volume Scheme", Ph.D. Thesis, Dept. of Aerospace and Ocean Engineering, Virginia Polytechnic Inst. and State Univ., Blacksburg, VA.

11. RESPONSIBILITY NOTICE

The author is the only responsible for the printed material included in this paper.